Developmental Biology 432 (2017) 258–264

Contents lists available at ScienceDirect

Developmental Biology

journal homepage: www.elsevier.com/locate/developmentalbiology

Distinct populations of embryonic epithelial progenitors generate Lgr5$^+$ intestinal stem cells

Margarita M. Dzama, Lira Nigmatullina, Sergi Sayols, Nastasja Kreim, Natalia Soshnikova*

Institute of Molecular Biology, D-55128 Mainz, Germany

ARTICLE INFO

Keywords:
Embryonic intestinal epithelial progenitors
Cellular heterogeneity
Lgr5$^+$ stem cell
Anterior-posterior patterning

ABSTRACT

The adult intestinal stem cells (ISCs) are transcriptionally heterogeneous. As the mechanisms governing their developmental specification are still poorly understood, whether this heterogeneity reflects an early determination of distinct cellular sub-types with potentially distinct physiological functions remains an open question. We investigate the cellular heterogeneity within the mouse embryonic midgut epithelium at the molecular and functional levels. Cell fate mapping analysis revealed that multiple early embryonic epithelial progenitors give rise to Lgr5$^+$ ISCs. The origin of the molecularly distinct early precursors along the anterior-posterior axis defines the transcriptional signature of embryonic Lgr5$^+$ ISC progenitors. We further show that the early epithelial progenitors have different capacity to generate Lgr5$^+$ ISC progenitors and Axin2$^+$ early precursors display the highest potential.

1. Introduction

The intestinal epithelium is the most vigorously self-renewing adult tissue. It is comprised of five differentiated cell types: enterocytes, goblet, Paneth, entero-endocrine and tuft cells (Beumer and Clevers, 2016). The distribution of different cell types varies greatly along the anterior-posterior axis of the intestinal tract supporting its diverse functions. For example, mucus producing goblet cells are generated in larger numbers in the posterior third, whereas more Paneth cells are produced in the anterior third of the small intestine (Iwasaki et al., 2011). Different subtypes of hormone producing entero-endocrine cells are also restricted to the specific regions along the anterior-posterior axis (Basak et al., 2017). Furthermore, many genes encoding digestive enzymes, ion, lipid and amino acid transporters are differentially expressed in absorptive enterocytes depending on their position along the small intestine (Anderle et al., 2005). The regional identity of the small intestinal epithelium is intrinsically encoded in intestinal epithelial stem cells (ISCs) (Fukuda et al., 2014; Middendorp et al., 2014).

To ensure the rapid turnover of the intestinal epithelium ISCs constantly divide and therefore express genes that promote their maintenance and proliferation (Beumer and Clevers, 2016). Many of the genes are the targets and mediators of the Wnt signalling pathway (Kretzschmar and Clevers, 2017). On the top of the gene list is *Lgr5* encoding a leucine-rich repeat containing, G-protein–coupled receptor (Barker et al., 2007), which strongly potentiates Wnt signalling (Carmon et al., 2011; de Lau et al., 2011; Glinka et al., 2011). *Axin2*, another target but a negative regulator of Wnt signalling (Behrens et al., 1998), is expressed in both ISCs and more differentiated progenies. Recently, we have shown that embryonic ISC progenitors also express many targets of Wnt signalling, including *Lgr5* and *Axin2* (Nigmatullina et al., 2017). A small population of the embryonic epithelial cells is specified as Lgr5 positive ISC progenitors around embryonic day 13.5 (E13.5). The cellular identity of the early epithelial precursors for Lgr5$^+$ ISC progenitors remains unknown.

In mice, the gut tube is formed around E9.0. It is composed of a single epithelial layer surrounded by mesenchyme. The epithelial lining of the midgut tube forms from the definitive and visceral endoderm (Kwon et al., 2008). Multiple transcription factors and signalling pathways, including Tgf-β/Bmp and Wnt, are essential for gut tube formation and patterning (Chin et al., 2017). Among those, the Foxa2 transcription factor plays an important role in specification of the definitive endoderm (Ang et al., 1993). It is expressed in the entire gut epithelium till E9.0 but gets restricted to the fore and hindgut around E9.5. Transient Wnt signalling, between E7.5 and E8.5, regulates patterning of the mid and hindgut (Sherwood et al., 2011). Activation of *Id2*, a target of the Tgf-β/Bmp pathway, in the intestinal epithelium blocks Wnt signalling by E9.5 (Nigmatullina et al., 2017). Id2 controls the time of ISC progenitor specification and their numbers during intestinal development till birth.

Dynamic transcriptional changes may generate molecular and functional heterogeneity within the developing midgut epithelium. Cells expressing the early endodermal marker *Foxa2* might have

* Corresponding author.
E-mail address: n.soshnikova@imb-mainz.de (N. Soshnikova).

http://dx.doi.org/10.1016/j.ydbio.2017.10.012
Received 21 August 2017; Received in revised form 4 October 2017; Accepted 12 October 2017
Available online 13 October 2017

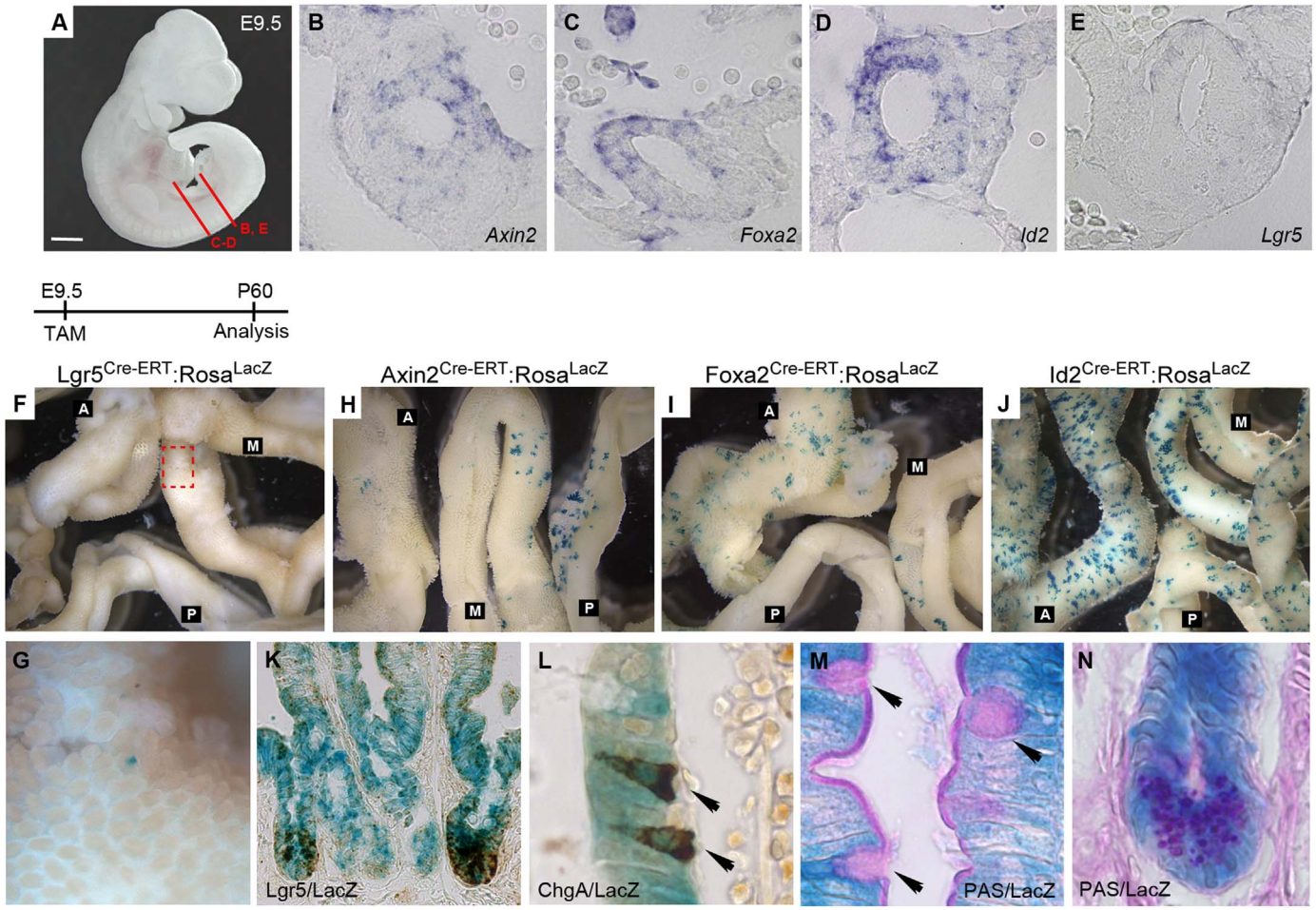

Fig. 1. Fate mapping of early embryonic intestinal epithelial progenitors. (**A**) Whole mount view of the mouse embryo at E9.5. Red lines show section levels for the corresponding images in (B-E). Expression of *Axin2* (**B**), *Foxa2* (**C**), *Id2* (**D**) and *Lgr5* (**E**) in the embryonic small intestine at E9.5 as revealed by RNA in situ hybridization. (**F-J**) Whole-mount view of LacZ stained *Lgr5*$^{EGFP\text{-}Cre\text{-}ERT}$:*Rosa26*^{lacZ} (**F**), *Axin2*$^{Cre\text{-}ERT}$:*Rosa26*^{lacZ} (**H**), *Foxa2*$^{Cre\text{-}ERT}$:*Rosa26*^{lacZ} (**I**) and *Id2*$^{Cre\text{-}ERT}$:*Rosa26*^{lacZ} (**J**) small intestines two months (P60) after a single treatment with tamoxifen (TAM) at E9.5 (n = 3 mice analysed), demonstrating the distribution and density of LacZ$^+$ clones along the anterior-posterior axis. Axin2$^+$ cells give rise to progenies mostly in the middle and posterior thirds of the small intestine. Foxa2$^+$ progenies contribute to the anterior third of the small intestine. A stands for the Anterior, M for the Middle and P for the Posterior small intestine. (**G**) Enlargement of the boxed area in "A" showing Lgr5:LacZ$^+$ clone. (**K-N**) Sections of LacZ stained small intestines from *Id2*$^{Cre\text{-}ERT}$/*Rosa26*^{lacZ} mice (n = 3 mice analysed), showing the distribution of Id2$^+$ progenies. (**K**) Immuno-labelling for GFP reveals Lgr5-EGFP$^+$ stem cells. (**L**) Staining for Chromogranin A (ChgA) shows entero-endocrine cells (arrowheads) surrounded by enterocytes within LacZ$^+$ (blue) villi. Co-staining with PAS shows goblet (pink, arrowheads, **M**) and Paneth cells (pink granules, **N**) positive for LacZ activity (blue). Scale bar: 0.5 mm (A), 10 μm (B-E), 1.7 mm (F, H-J), 0.4 mm (G), 15 μm (K) and 4 μm (L-N).

different functions compared to Wnt signalling positive or Id2$^+$ cells. To test this hypothesis we followed the fates of the cells expressing *Axin2*, *Foxa2* and *Id2* using lineage tracing analysis. We found that Axin2$^+$ early progenitors have a higher capacity to specify as Lgr5$^+$ cells during embryogenesis. However, the potential to generate Lgr5$^+$ cells is not restricted to Axin2$^+$ progenitors at E9.5. Further transcriptome profiling revealed that the molecular signatures of Lgr5$^+$ cells specified from different progenitors reflect their location along the anterior-posterior axis.

2. Results

2.1. Multiple embryonic epithelial cells contribute to the adult ISC pool

To define early embryonic intestinal epithelial progenitors we performed genetic lineage-tracing analysis using mouse lines, which express a tamoxifen-inducible *Cre* transgene from endogenous gene loci. We first analysed the expression patterns of *Axin2*, *Foxa2*, *Id2* and *Lgr5* within the embryonic midgut at E9.5 (Fig. 1A). Specifically, *Axin2*, a target of the Wnt pathway, was weakly expressed in a subset of epithelial and mesenchymal gut cells (Fig. 1B). The expression of *Axin2* was stronger in the posterior compared to the anterior midgut epithelium. Few *Foxa2* positive cells were detected in the anterior midgut epithelium (Fig. 1C). Moreover, *Foxa2* expression was restricted to the dorsal midgut epithelium. *Id2*, a negative regulator of Wnt signalling (Nigmatullina et al., 2017), showed a broader expression pattern in both epithelium and mesenchyme (Fig. 1D). *Id2* expression domain encompassed the whole midgut tube with slight gradient of expression, high levels rostral and lower levels caudally. Consistent with our previous observations (Nigmatullina et al., 2017), *Lgr5* expression was not detected in the midgut at E9.5 (Fig. 1E). Together, our data show that the expression levels of *Axin2*, *Foxa2* and *Id2* vary between the intestinal epithelial cells at E9.5.

In order to study progenitor potential of the midgut epithelial cell populations *Axin2*$^{Cre\text{-}ERT}$:*Rosa26*^{lacZ} (Bowman et al., 2013), *Foxa2*$^{Cre\text{-}ERT}$:*Rosa26*^{lacZ} (Park et al., 2008), *Id2*$^{Cre\text{-}ERT}$:*Rosa26*^{lacZ} (Rawlins et al., 2009) and *Lgr5*$^{Cre\text{-}ERT}$:*Rosa26*^{lacZ} (Barker et al., 2007) embryos were subjected to a single tamoxifen pulse at E9.5, and the small intestines were analysed for LacZ expression 2 months later. Of note, our labelling protocol yields over 95% of labelled cells using *Rosa26*$^{Cre\text{-}ERT}$ driver (Supplementary Fig. S1A and Nigmatullina et al., 2017). We have observed a few LacZ positive clones (4 ± 1, n = 3), confined to a few crypts in the most anterior part of the *Lgr5*$^{Cre\text{-}ERT}$:*Rosa26*^{lacZ} small

intestines (Fig. 1F-G). In contrast, we detected multiple LacZ positive clones in the *Axin2*$^{Cre-ERT}$:*Rosa26*^{lacZ} small intestines (Fig. 1H), indicating that Axin2$^+$ cells are early progenitors of the adult ISCs. Furthermore, the analysis of *Foxa2*$^{Cre-ERT}$:*Rosa26*^{lacZ} mice also revealed multiple LacZ positive clones (Fig. 1I). Foxa2$^+$ descendants were present only in the anterior third of the small intestine, whereas Axin2$^+$ progenies were found mostly in the middle and posterior parts. In agreement with *Id2* expression domain, around 20% of villi in *Id2*$^{Cre-ERT}$:*Rosa26*^{lacZ} small intestine were LacZ positive (Fig. 1J). Moreover, a larger amount of LacZ$^+$ clones was observed in the anterior third of the small intestine in *Id2*$^{Cre-ERT}$ mice. LacZ$^+$ clones consisted of Lgr5$^+$ adult stem cells as well as all differentiated intestinal epithelial cell types, including enterocytes, chromogranin A positive entero-endocrine, goblet and Paneth cells (Fig. 1K-N). These findings indicate that different embryonic epithelial precursors contribute to the adult ISCs.

2.2. *Axin2*$^+$ *early progenitors are prone to specify into Lgr5*$^+$ *cells*

In lineage tracing studies, there are at least two parameters defining the number of labelled clones in a tissue. The first is the number of *Cre-ERT* expressing cells at the time of labelling. The second is the progenitor potential (stemness) of the labelled cells. To assess the ability of the early embryonic epithelial cells to give rise to Lgr5$^+$ progenitors, we used *Rosa26*^{tdTomato} and *Lgr5*$^{EGFP-Cre-ERT}$ reporters to simultaneously visualize lineage-traced progenies and GFP labelled Lgr5$^+$ cells. We treated *Axin2*$^{Cre-ERT}$:*Rosa26*^{tdTomato}:*Lgr5*$^{EGFP-Cre-ERT}$, *Foxa2*$^{Cre-ERT}$:*Rosa26*^{tdTomato}:*Lgr5*$^{EGFP-Cre-ERT}$, *Id2*$^{Cre-ERT}$:*Rosa26*^{tdTomato}:*Lgr5*$^{EGFP-Cre-ERT}$ and *Lgr5*$^{EGFP-Cre-ERT}$:*Rosa26*^{tdTomato} embryos with tamoxifen at E9.5 and performed FACS analysis at E13.5, the time of Lgr5$^+$ progenitor specification (Fig. 2A and Nigmatullina et al., 2017). To label specifically epithelial cells we used pan-endodermal marker EpCAM (Supplementary Fig. S1B-C). 8.4 ± 0.5% of Lgr5-EGFP$^+$ cells were detected in *Lgr5*$^{EGFP-Cre-ERT}$:*Rosa26*^{tdTomato} embryonic small intestine at E13.5 (Fig. 2C-D and Supplementary Fig. S2A). Consistent with the small number of Lgr5$^+$LacZ$^+$ clones in the adult small intestine, we have observed less than 5 Lgr5-EGFP$^+$tdTomato$^+$ cells in those embryos (Fig. 2E). Yet, all tdTomato$^+$ cells were Lgr5-EGFP positive (Fig. 2B).

The analysis of *Axin2*$^{Cre-ERT}$:*Rosa26*^{tdTomato}:*Lgr5*$^{EGFP-Cre-ERT}$ embryos revealed that out of 11 ± 2.2% of Axin2 progenies 1.94 ± 0.7% were also Lgr5-EGFP positive (Fig. 2F-G), indicating that Axin2$^+$ progenitors (Axin2:tdTomato$^+$) have slight (1.8 times) but significantly (P = 0.002, Student´s *t*-test) increased frequency to generate Lgr5$^+$ embryonic progenitors compared to Axin2$^-$ cells (Fig. 2B). In contrast, out of 6.9 ± 1% of Foxa2:tdTomato$^+$ cells 0.52 ± 0.08% were also Lgr5-EGFP$^+$ (Fig. 2H-I) in *Foxa2*$^{Cre-ERT}$:*Rosa26*^{tdTomato}:*Lgr5*$^{EGFP-Cre-ERT}$ embryos, suggesting that Lgr5$^+$ cells are specified at random either from Foxa2$^+$ or Foxa2$^-$ cells (Fig. 2B). Moreover, in agreement with the function of *Id2* as a negative regulator of Wnt signalling (Nigmatullina et al., 2017), twice less (Fig. 2B, P = 0.002, Student's *t*-test) Lgr5$^+$ cells were specified from Id2$^+$ compared to Id2$^-$ progenitors (6.8 ± 0.52% of Id2:tdTomato$^+$Lgr5-EGFP$^+$ out of 57.7 ± 3% Id2:tdTomato$^+$ cells) (Fig. 2J-K). Taken together, our data show that early Axin2$^+$ epithelial cells have higher capability to specify in late Lgr5$^+$ embryonic progenitors, when compared to Axin2$^-$ or to the other cell populations examined. This suggests than *Axin2* is an early marker for intestinal stem cell progenitors during intestinal development, which might be due to the higher levels of Wnt signalling in Axin2$^+$ cells.

2.3. *Unifying transcriptional signature for Lgr5*$^+$ *progenitors of different origin*

Gene expression analysis of the embryonic intestinal epithelium revealed that Lgr5$^+$ progenitors have a distinct molecular signature compared to Lgr5$^-$ epithelial cells at E13.5 (Nigmatullina et al., 2017). To determine how similar are Lgr5$^+$ progenitors of different origins we sequenced the transcriptomes of FACS purified Lgr5$^+$ cells derived either from Axin2$^+$ (Axin2:tdTomato$^+$Lgr5$^+$EpCAM$^+$) or from Id2$^+$ (Id2:tdTomato$^+$Lgr5$^+$EpCAM$^+$) or from Axin2$^-$ and Id2$^-$ (Lgr5$^+$EpCAM$^+$) progenitors, as well as control embryonic epithelial cells (Axin2:tdTomato$^+$EpCAM$^+$, Id2:tdTomato$^+$EpCAM$^+$ and EpCAM$^+$) from the small intestine at E13.5, after tamoxifen treatment at E9.5 (Fig. 2G, K). Around 600 differentially expressed genes were identified between Lgr5$^+$EpCAM$^+$ and Lgr5$^-$EpCAM$^+$ cells (log_2FC ≥ 0.5, FDR < 0.01, RPKM ≥ 100, Fig. 3A and Supplementary Tables S1-S2). The Wnt responsive genes were upregulated whereas differentiation associated genes were downregulated in Lgr5$^+$EpCAM$^+$ compared to the control cells, thus defining a *bona fide* ISC progenitor signature (Fig. 3B).

Comparative analysis of Axin2:tdTomato$^+$Lgr5$^+$EpCAM$^+$ and Lgr5$^+$EpCAM$^+$ defined around 200 differentially expressed genes (log_2FC ≥ 0.5, FDR < 0.01, RPKM ≥ 100, Fig. 3A-C and Supplementary Tables S3-S4), suggesting that Lgr5$^+$ progenitors derived from Axin2$^+$ and Axin2$^-$ precursors have distinct molecular signatures. 88% of differentially expressed genes were upregulated in Axin2:tdTomato$^+$Lgr5$^+$EpCAM$^+$ compared to Lgr5$^+$EpCAM$^+$ cells (Fig. 3C). Interestingly, *Id2* was between the few genes expressed at lower levels in Axin2:tdTomato$^+$Lgr5$^+$EpCAM$^+$ compared to Lgr5$^+$EpCAM$^+$ cells. Yet, the expression of Wnt targets or markers of differentiation was similar among the two cell populations (Fig. 3B).

Surprisingly, we found only 1 gene as differentially expressed between Id2:tdTomato$^+$Lgr5$^+$EpCAM$^+$ and Lgr5$^+$EpCAM$^+$ cells (log_2FC ≥ 0.5, FDR < 0.01, RPKM ≥ 100, Fig. 3A-B), indicating that Lgr5$^+$ progenitors derived from Id2$^+$ and Id2$^-$ precursors are identical. Further analysis of Id2:tdTomato$^+$EpCAM$^+$ and EpCAM$^+$ cells showed only 9 differentially expressed genes (log_2FC ≥ 0.5, FDR < 0.01, RPKM ≥ 100, Fig. 3A and Supplementary Tables S7-S8), with *Sfrp5, Onecut2* and *St8sia3* being higher expressed in Id2:tdTomato$^+$EpCAM$^+$ compared to EpCAM$^+$ cells (Fig. 3B). In contrast, the same genes were expressed at lower levels in Axin2:tdTomato$^+$EpCAM$^+$ compared to EpCAM$^+$ cells (Fig. 3A-B and Supplementary Tables S5-S6). Of note, *Sfrp5, Onecut2, St8sia3* and *Fabp1* genes are expressed at higher levels in the anterior half of the small intestine compared to the posterior part (Wang et al., 2015; Nigmatullina et al., 2017). These short list of differentially expressed genes suggests that the slight differences detected between Id2:tdTomato$^+$EpCAM$^+$, Axin2:tdTomato$^+$EpCAM$^+$ and EpCAM$^+$ cell populations are due to their different distribution along the anterior-posterior axis, with the higher number of Id2:tdTomato$^+$EpCAM$^+$ cells in the anterior part and Axin2:tdTomato$^+$EpCAM$^+$ cells in the posterior part of the small intestine.

To test this hypothesis, we FACS purified Axin2:tdTomato$^+$Lgr5$^+$EpCAM$^+$, Axin2:tdTomato$^+$EpCAM$^+$, Lgr5$^+$EpCAM$^+$ and EpCAM$^+$ cells from the embryonic small intestine at E15.5 after tamoxifen treatment at E9.5 (Fig. 4 and Supplementary Fig. S2B). Our FACS analysis revealed few (0.29 ± 0.19%) Axin2:tdTomato$^+$Lgr5$^+$EpCAM$^+$ cells in the anterior half of the small intestine (Fig. 4A, C). In contrast, 6 ± 2% of Axin2$^+$ cells was also Lgr5 positive in the posterior part of the small intestine at E15.5 (Fig. 4B, D). This indicates that the majority of the double positive cells are located in the posterior small intestine. Therefore, we have analysed the transcriptomes of the cells isolated from the posterior small intestines. We found only 2 genes as differentially expressed (log_2FC ≥ 0.5, FDR < 0.01, RPKM ≥ 100, Fig. 4E) between Axin2:tdTomato$^+$Lgr5$^+$EpCAM$^+$ and Lgr5$^+$EpCAM$^+$ cells. Further comparison between the posterior Axin2:tdTomato$^+$Lgr5$^+$EpCAM$^+$ and the anterior Lgr5$^+$EpCAM$^+$ revealed 250 differentially expressed genes (log_2FC ≥ 0.5, FDR < 0.01, RPKM ≥ 100, Fig. 4E and Supplementary Tables S9-S10). Therefore, we conclude that Lgr5$^+$ embryonic cells specified from different progenitors have very similar transcriptional signature with differences reflecting their position along the anterior-posterior axis.

Interestingly, we identified around 80 differentially expressed genes (log_2FC ≥ 0.5, FDR < 0.01, RPKM ≥ 100, Fig. 4F and Supplementary Tables S11-S14) between Axin2:tdTomato$^+$EpCAM$^+$ and EpCAM$^+$ cells

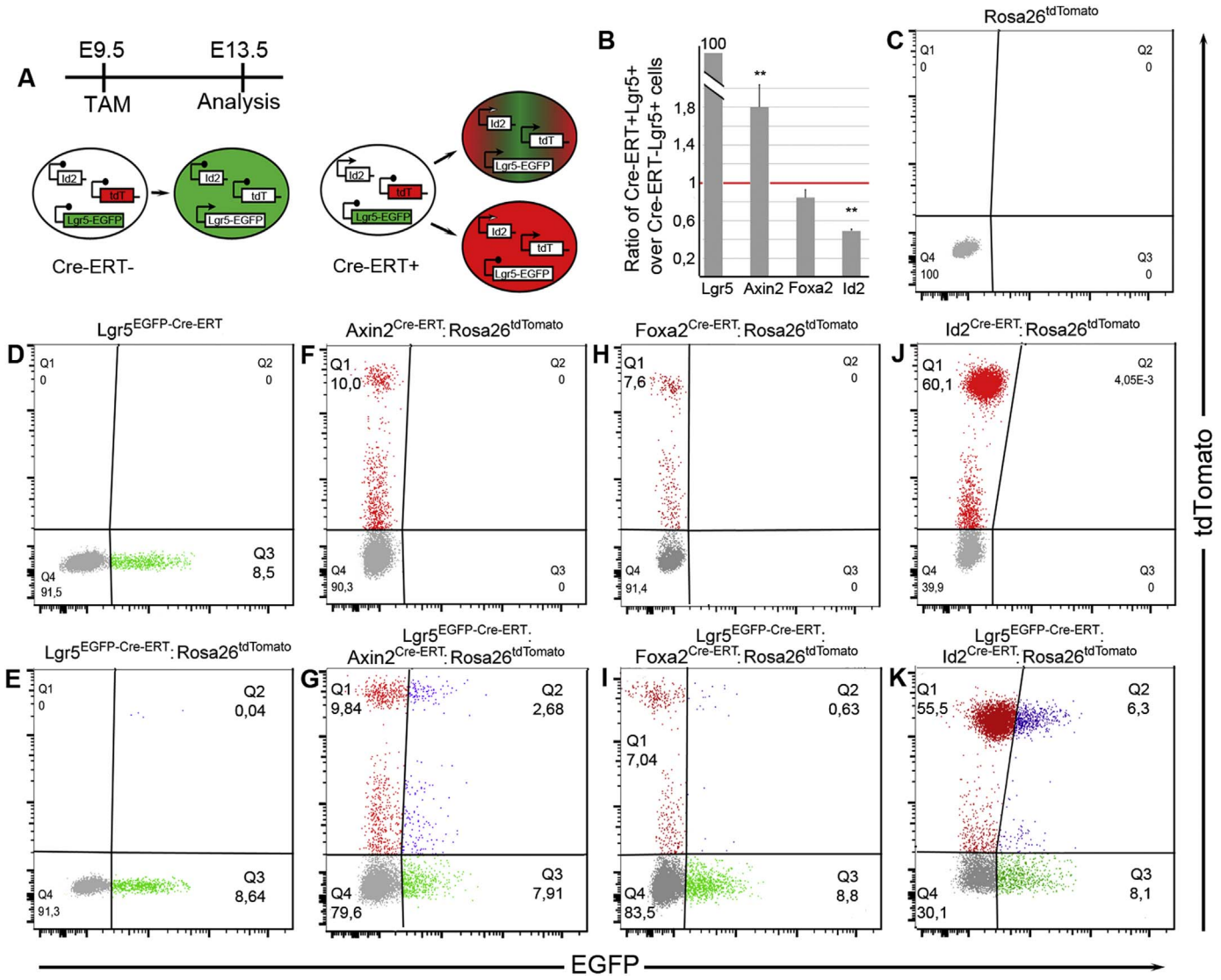

Fig. 2. Embryonic intestinal progenitors have different capacity to specify into Lgr5$^+$ progenitors. (**A**) Possible outcomes of lineage tracing assay. Cells expressing *Cre* activate *tdTomato* reporter (red) upon TAM administration at E9.5 and give rise to permanently labelled progeny (red). Due to the temporal difference for Axin2, Foxa2, Id2- and Lgr5-Cre-ERT activity only the progenies of Axin2$^+$, Foxa2$^+$ or Id2$^+$ cells could be labelled in red upon treatment with TAM at E9.5. Two types of Id2$^+$ progenies can be observed: double positive Id2$^+$:Lgr5-EGFP$^+$ (both red and green, top) and Id2$^+$Lgr5-EGFP$^-$ (red, bottom). *Cre* negative cells expressing *Lgr5-EGFP* are labelled in green at E13.5. (**B**) Ratios between the numbers of Lgr5$^+$ cells specified either from Cre-ERT$^+$ or Cre-ERT$^-$ progenitors. Error bars are ± SD, (n = 4). $^{**}P < 0.01$ by Student´s *t*-test. (**C-K**) Representative FACS plots showing EpCAM$^+$ (grey, Q4), Lgr5-EGFP$^+$EpCAM$^+$ (green, Q3), Axin2-Cre-ERT:tdTomato$^+$EpCAM$^+$ (red, Q1, F-G), Foxa2-Cre-ERT:tdTomato$^+$EpCAM$^+$ (H-I), or Id2-Cre-ERT:tdTomato$^+$EpCAM$^+$ (J-K), and double positive Lgr5-EGFP-Cre-ERT:tdTomato$^+$EpCAM$^+$ (purple, Q2, D-E), Axin2-Cre-ERT:tdTomato$^+$Lgr5-EGFP$^+$EpCAM$^+$ (F-G), Foxa-Cre-ERT:tdTomato$^+$Lgr5-EGFP$^+$EpCAM$^+$ (H-I), Id2-Cre-ERT:tdTomato$^+$Lgr5-EGFP$^+$EpCAM$^+$ (J-K) cell populations isolated from the embryonic small intestine at E13.5, four days after a single treatment with TAM (n = 4 embryos analysed).

at E15.5. The expression of Wnt target genes, including *Lgr5*, *Smoc2* and *Slc12a2*, as well as of the genes belonging to the secretory lineage (Basak et al., 2014), such as *Atoh1*, *Spdef*, *Neurog3*, *Dll1* and *Reg4*, was specifically increased in Axin2:tdTomato$^+$EpCAM$^+$ compared to EpCAM$^+$ cells, suggesting that they could represent early common secretory progenitors.

3. Discussion

The embryonic origin of many adult stem cells remains elusive. We have recently shown that Lgr5$^+$ intestinal stem cell progenitors are specified late during embryogenesis and represent only a minor fraction of the intestinal epithelium (Nigmatullina et al., 2017). The early embryonic intestinal epithelial cells can be specified in Lgr5$^+$ cells in response to external Wnt signals and/or a certain pool of early progenitors can be poised for the robust activation of Wnt dependent transcriptional program, for example at the level of chromatin. Here, we show that multiple early embryonic epithelial progenitors give rise to Lgr5$^+$ cells. The capacity to generate Lgr5$^+$ ISC progenitors is high in early Axin2$^+$ precursors and low in Id2$^+$ cells. Nevertheless, once specified, Lgr5$^+$ progenitors display the ISC transcriptional signature independent of their origin. They could be distinguished, however, based on their position along the anterior-posterior axis.

The early midgut epithelium is comprised of heterogeneous cell populations. On one hand, the epithelial cells have different transcriptional signatures according to their positions along the anterior-posterior axis. For example, Foxa2$^+$ progenitors are located in the anterior part, and Axin2$^+$ cells are positioned in the posterior half of the small intestine. On the other hand, there is heterogeneity in the levels of Wnt signalling within the midgut epithelium. Axin2$^+$ cells represent a population with higher Wnt dependent transcriptional activity compared to Id2$^+$ cells. Does this transcriptional heterogeneity translate into functional heterogeneity? Our data show that Axin2$^+$ early progenitors have a 4 times higher capacity to generate Lgr5$^+$ ISC

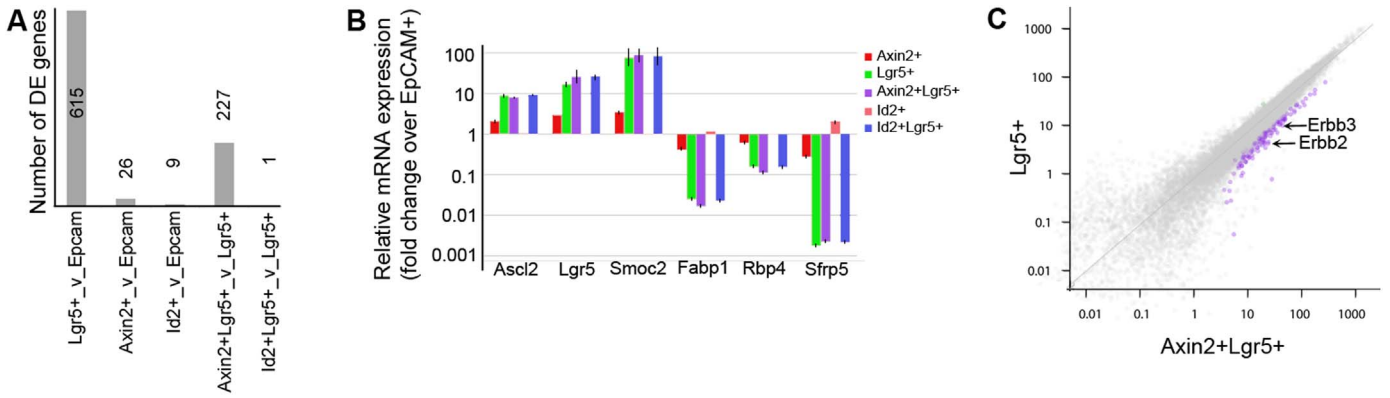

Fig. 3. Gene expression analysis of Lgr5$^+$ progenitor populations. (**A**) The number of differentially expressed genes between indicated cell populations isolated by FACS at E13.5 as defined by RNA-sequencing analysis. (**B**) Quantitative RT-PCR analysis for selected stem cell (*Ascl2, Lgr5* and *Smoc2*) or differentiation (*Sfrp5, Rbp4* and *Fabp1*) markers in Axin2-Cre-ERT:tdTomato$^+$EpCAM$^+$ (red), Lgr5-EGFP$^+$EpCAM$^+$ (green), Axin2-Cre-ERT:tdTomato$^+$EpCAM$^+$ (purple), Id2-Cre-ERT:tdTomato$^+$EpCAM$^+$ (pink) and Id2-Cre-ERT:tdTomato$^+$Lgr5-EGFP$^+$EpCAM$^+$ (blue) compared to the control EpCAM$^+$ cells. Data show relative expression levels for each gene, as compared to EpCAM$^+$ cells. Relative expression levels of each gene in EpCAM$^+$ were fixed to 1. Error bars are ± SD, (n = 3). (**C**) FPKM scatter plot illustrating gene expression profiles of Lgr5$^+$EpCAM$^+$ (y-axis) and Axin2$^+$Lgr5-EGFP$^+$EpCAM$^+$ (x-axis) cells. Genes expressed at higher levels in Axin2$^+$Lgr5-EGFP$^+$EpCAM$^+$ progenies compared to Lgr5$^+$EpCAM$^+$ cells ($\log_2 \geq 1$, FDR < 0.01) are in purple. Genes expressed at higher levels in Lgr5$^+$EpCAM$^+$ compared to Axin2$^+$Lgr5-EGFP$^+$EpCAM$^+$ cells ($\log_2 \geq 1$, FDR < 0.01) are in blue. Non-differentially expressed transcripts as well as those detected below 0.5 FPKM in both samples are in grey.

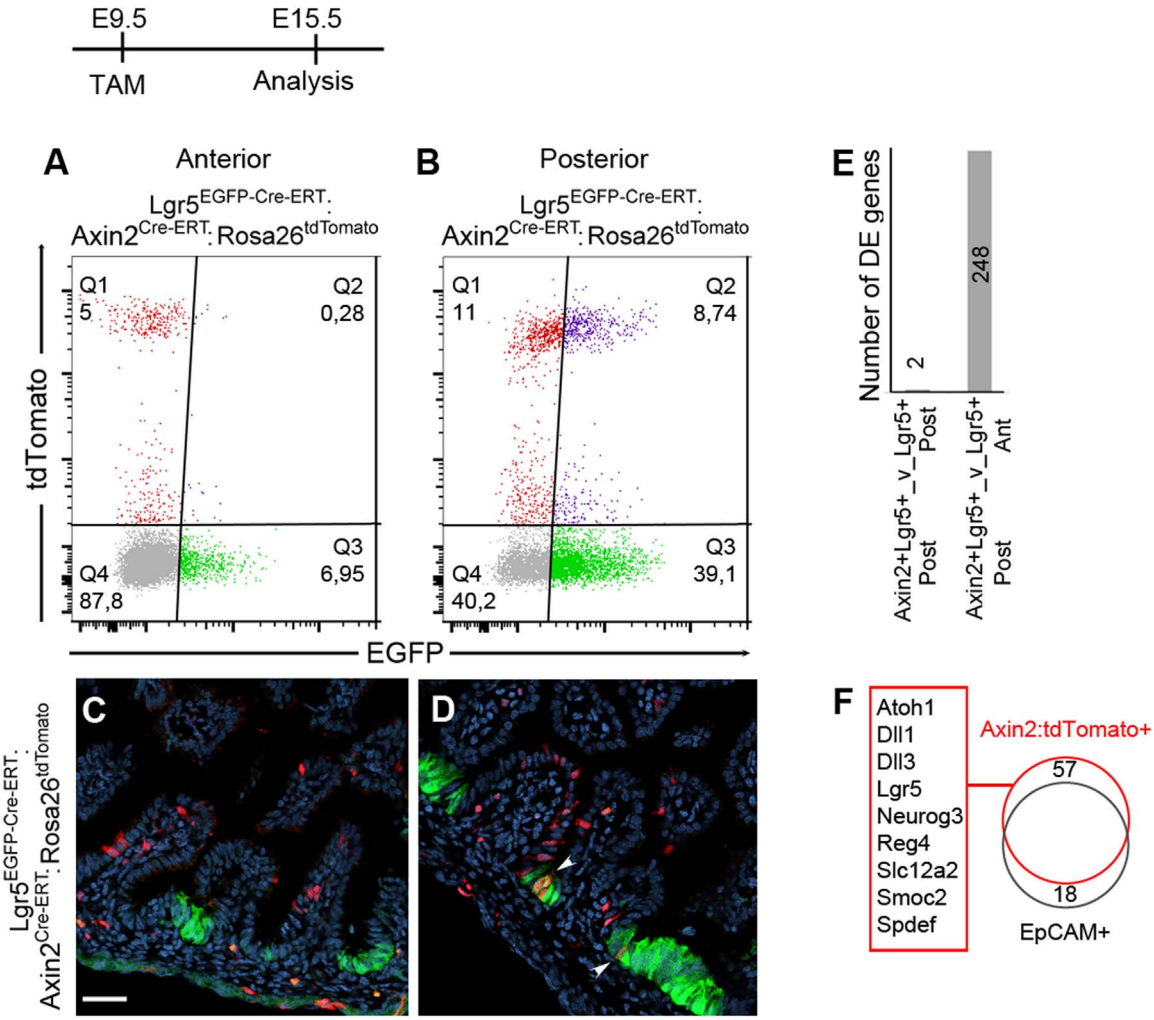

Fig. 4. Transcriptional signatures of Axin2$^+$ progenies. (**A-B**) Representative FACS plots showing EpCAM$^+$ (grey, Q4), Lgr5-EGFP$^+$EpCAM$^+$ (green, Q3), Axin2-Cre-ERT:tdTomato$^+$EpCAM$^+$ (red, Q1) and double positive Axin2-Cre-ERT:tdTomato$^+$Lgr5-EGFP$^+$EpCAM$^+$ (purple, Q2), cell populations isolated from either the anterior (**A**) or the posterior (**B**) halves of the embryonic small intestine at E15.5, six days after a single treatment with TAM (n = 6 embryos analysed). (**C-D**) Sections of the anterior (**C**) and the posterior (**D**) halves of the small intestines from *Axin2$^{Cre\text{-}ERT}$:Lgr5$^{EGFP\text{-}Cre\text{-}ERT}$:Rosa26^{tdTomato}* embryos co-stained with EGFP antibody showing distribution of Axin2-Cre-ERT:tdTomato$^+$ progenies (red) and Lgr5-EGFP$^+$ cells (green) at E15.5 after a single treatment with TAM at E9.5. Double positive Axin2-Cre-ERT:tdTomato$^+$Lgr5-EGFP$^+$ cells (white arrowheads) reside within the inter-villi compartment. Scale bar: 20 μm. (**E**) The number of differentially expressed genes between indicated cell populations isolated by FACS at E15.5 as defined by RNA-sequencing analysis. (**F**) Venn diagram showing the number of differentially expressed genes between Axin2-Cre-ERT:tdTomato$^+$EpCAM$^+$ (red) and EpCAM$^+$ (grey) cells.

progenitors than Id2$^+$ cells. This characteristic of Axin2$^+$ early progenitors could be related to the increased Wnt dependent transcriptional activity, and to a distinct chromatin state. Indeed, many of Wnt responsive ISC signature genes, including *Axin2*, are targets of DNA methylation dependent mechanisms in Lgr5$^-$ embryonic intestinal epithelial cells (Kazakevych et al., 2017). Of note, *Id2$^{Cre\text{-}ERT}$* embryos express only one functional copy of *Id2*, which results in two-fold increase in Lgr5$^+$ ISC progenitors at E13.5 (Fig. 2K and Nigmatullina et al., 2017). It is thus possible that in the presence of both functional *Id2* alleles, even less Lgr5$^+$ progenitors could be specified from Id2$^+$ cells. Furthermore, we cannot rule out that some Id2$^+$ progenitors also express *Axin2* in the posterior midgut epithelium. Therefore, the functional difference between Axin2$^+$ and Id2$^+$ progenitors is likely underestimated in our experimental setup.

Axin2$^+$ progenies express *Lgr5* at intermediate levels between Axin2$^+$Lgr5$^+$ and Axin2$^-$Lgr5$^-$ cells at E13.5. Later during development, markers of label-retaining secretory progenitors or "reserve" ISCs (Basak et al., 2014), including *Dll1, Dll4, Foxa3, Kit, Lrig1, Neurog3, Pax4* and *Reg4*, are expressed at significantly higher levels in Axin2$^+$Lgr5$^-$ compared to Axin2$^-$Lgr5$^-$ progenies. This suggests that either Axin2$^+$ early progenitors have a higher capacity to generate label-retaining secretory precursors or they specify into secretory precursors earlier than Axin2$^-$ progenies. Further studies will be required to understand the mechanisms underlying the functional characteristics of Axin2$^+$ early progenitors.

Our data demonstrate that Lgr5$^+$ ISC progenitors are specified from various cell populations. The embryonic intestinal epithelium is a vigorously expanding tissue, which constantly receives signals from a heterogeneous population of mesenchymal cells. Generation of a large progenitor pool, which commits to Lgr5$^+$ cell fate late during embryogenesis, might be necessary to reduce transcriptional variability between ISC progenitors as well as to ensure their constant numbers between embryos. Indeed, with the exception of their regional anterior-posterior identity, Lgr5$^+$ progenitors of different origins have identical transcriptional profiles. In summary, our study supports a model in which the embryonic midgut epithelium contains multiple molecularly and functionally distinct progenitors of Lgr5$^+$ ISCs. The regional differences between early embryonic progenitors are further inherited and maintained by adult ISCs, which is essential for the generation of physiological diversity along the anterior-posterior axis of the small intestine. Further studies revealing the contribution of distinct embryonic progenitors in neoplastic lesions will be important for our understanding of the mechanisms of cancer initiation.

4. Experimental procedures

4.1. Mice

Lgr5$^{EGFP\text{-}Cre\text{-}ERT}$, *Id2$^{Cre\text{-}ERT}$*, *Axin2$^{Cre\text{-}ERT}$*, *Foxa2$^{Cre\text{-}ERT}$*, *Rosa26^{tdTomato}* and *Rosa26^{lacZ}* mice were obtained from Jackson laboratory. CD1 mice were from Charles Rivers. Tamoxifen (Sigma) was administered via oral gavage at 0.12 mg/g dam body weight. When P60 stage was required, newborn mice were fed by adoptive lactating CD1 females. Mouse colonies were maintained in a certified animal facility in accordance with European guidelines. These experiments were approved by the local ethical committee.

4.2. RNA in situ hybridization

Embryos were fixed overnight in 4% formaldehyde in PBS at 4 °C, dehydrated through the series of MetOH and treated for 15 min with 6% H_2O_2. After rehydration, embryos were treated for 10 min with 20 μg/ml proteinase K, post-fixed with 4% formaldehyde for 15 min, equilibrated with 5x SSC in 50% Formamid and hybridized overnight at 63 °C with digoxygenin labelled RNA probes for *Axin2, Foxa2, Id2* and *Lgr5*. Sections were washed and incubated overnight with sheep anti-digoxygenin antibody 1:3000 (Roche). At least three independent biological replicates were used for each experiment. Images were acquired with Leica DM2500 microscope.

4.3. Histological techniques

Embryonic or adult small intestines were dissected, fixed for 20 min in 1% formaldehyde in PBS at 4 °C, incubated overnight in 30% sucrose, embedded in OCT and kept at −80 °C. Immunohistochemical analyses were performed on 10 μm cryosections using anti-Chromogranin A 1:1000 (rabbit, ImmunoStar Inc.) followed by Vectastain Elite ABC kit (Vector Laboratories) according to the manufacturer's instructions. Counterstaining of nuclei was performed with DAPI 1:1000 (Sigma). Lgr5-EGFP was detected using anti-GFP antibody 1:1000 (Thermofisher) followed by Alexa488-conjugated goat anti-rabbit antibody 1:2000 (Invitrogen). Periodic Acid Schiff staining was performed according to the manufacturer's instructions (Sigma).

To detect LacZ$^+$ cells small intestines were dissected in PBS, fixed with 0,2% glutaraldehyde for 20 min, washed 3 times with PBS/ 0.01% NP-40/ 0.01% Na-deoxycholate and incubated for 4 h in staining solution (5 mM $K_3[Fe(CN)_6]$, 5 mM $K_4[Fe(CN)_6]$, 2 mM $MgCl_2$, 0.01% NP-40, 0.01% Na-deoxycholate and 1 mg/ml X-gal in PBS). Three independent biological replicates were used for each experiment. Images were acquired with Leica DM2500, M205FA and confocal SPE microscopes.

4.4. Isolation of embryonic intestinal epithelial cells using flow cytometry

Small intestines were dissected from mouse embryos at indicated stages, cut in pieces of 2 mm and incubated for 5–10 min with 0.15 mg/ml collagenase (Sigma) in PBS at 37 °C with shaking at 800 rpm. Single cell suspensions were collected by centrifugation at 200*g* for 3 min, washed twice and resuspended in PBS supplemented with 2% goat serum. Cells were stained with APC–conjugated anti-EpCAM 1:1000 (eBioscience) antibody for 15 min at room temperature. Living cells were gated by DAPI dye exclusion. Embryonic intestinal epithelial cells were isolated as EpCAM$^+$DAPI$^-$. Embryonic Lgr5$^+$ cells were isolated as EGFP$^+$EpCAM$^+$DAPI$^-$. Fluorescence-activated cell sorting analysis was performed using BD FACS Aria II SORP cell sorter (85 μM nozzle) and FlowJo software.

4.5. Low cell number RNA-sequencing

For ultralow cell number RNA-sequencing two hundred fifty Axin2:tdTomato$^+$Lgr5-EGFP$^+$EpCAM$^+$, Axin2:tdTomato$^+$EpCAM$^+$, Id2:tdTomato$^+$Lgr5-EGFP$^+$EpCAM$^+$, Id2:tdTomato$^+$EpCAM$^+$, Lgr5-EGFP$^+$EpCAM$^+$ and EpCAM$^+$ embryonic intestinal cells were isolated by FACS directly in 7μl of lysis buffer (Clontech) supplemented with 5% RNase inhibitor and stored at −80 °C. For each replicate (n = 3), RNA was isolated from pool of 2–3 embryos. PolyA$^+$ mRNA was used for cDNA synthesis using SMARTer v2.0 kit (Clontech) according to the manufacturer's instructions. Amplification was performed for 15 cycles. After cDNA fragmentation (Covaris), libraries were prepared using Ovation Ultralow Library System (NuGEN) according to the manufacturer's instructions. Three independent FACS, cDNA synthesis, library preparations and sequencing experiments were performed.

4.6. RNA-sequencing data analysis

Raw reads were pre-processed and the quality was assessed with FastQC (http://www.bioinformatics.bbsrc.ac.uk/projects/fastqc). Reads were mapped to the iGenomes (http://support.illumina.com/sequencing/sequencing_software/igenome.html) UCSC mouse genome reference version mm9 using STAR (Dobin et al., 2013) version 2.3.1z13_r470 as the aligner, allowing up to two mismatches

and keeping only the primary reads, and the minimum intron size set to 10 nucleotides. The junctions' database for the STAR reference was built with the gene model from the iGenomes, downloaded from UCSC on March 6th, 2013. Reads falling on features were counted with the HTSeq-count (Anders et al., 2015) software, using the same gene model used before to guide the aligner, and handling overlapping reads in the default *union* mode. For the differential expression analysis, we used R version 3.3.2 (R Core Team, 2017) and DESeq. 2 version 1.14.1 (Love et al., 2014) to normalize, transform, and model the data. The counts were fitted to a Negative Binomial generalized linear model (GLM) and the Wald significance test was used to determine the differentially expressed genes between various epithelial cell populations. Finally, RPKM values were calculated per gene using the library size-normalized FPM (robust counts per million mapped fragments) values from DESeq. 2 and multiplying them by 1000 divided by the gene length. The sequencing data have been deposited in the NCBI Gene Expression Omnibus database.

4.7. Quantitative PCR

For qPCR, 10 ng of cDNA from $Axin2^{Cre\text{-}ERT}$:$tdTomato^{+}Lgr5$-$EGFP^{+}EpCAM^{+}$, $Axin2^{Cre\text{-}ERT}$:$tdTomato^{+}EpCAM^{+}$, $Id2^{Cre\text{-}ERT}$:$tdTomato^{+}Lgr5$-$EGFP^{+}EpCAM^{+}$, $Id2^{Cre\text{-}ERT}$:$tdTomato^{+}EpCAM^{+}$, $Lgr5$-$EGFP^{+}EpCAM^{+}$, $EpCAM^{+}$ embryonic intestinal cells were used. Expression changes were then normalized to *Epcam*. PCR primers were designed using Primer Blast (http://www.ncbi.nlm.nih.gov/tools/primer-blast/) or qPCR Primers software from UCSC genome browser (http://genome.ucsc.edu). PCR was performed using SYBR green containing master mix kit (Applied Biosystems) with ViiA™ 7 cycler (Applied Biosystems). A mean quantity was calculated from triplicate reactions for each sample.

Acknowledgements

We thank I. Schaefer and S. Bürger (Cytometry platform), M. Mendez-Lago, C. Werner and H. Lukas (Genomics platform), S. Ritz, J. Schwirtz and M. Hanulova (Microscopy platform), J. Klassek and J. Geisinger for help, K. Weiser and T. Dehn for assistance with mouse breeding and T. Montavon for valuable comments on the manuscript. This work was funded by the Boehringer Ingelheim Foundation.

Author contributions

M.M.D. and L.N. performed experiments and analysed the data; S.S. and N.K. performed analyses of RNA-sequencing data; N.S. designed the study, performed experiments, analysed the data and wrote the manuscript with inputs from all authors.

Author information

The data discussed in this publication have been deposited in GEO database under accession number GSE104727. The authors declare no competing financial interests. Correspondence and requests for materials should be addressed to N.S. (n.soshnikova@imb-mainz.de).

Appendix A. Supporting information

Supplementary data associated with this article can be found in the online version at doi:10.1016/j.ydbio.2017.10.012.

References

Anderle, P., Sengstag, T., Mutch, D.M., Rumbo, M., Praz, V., Mansourian, R., Delorenzi, M., Williamson, G., Roberts, M.A., 2005. Changes in the transcriptional profile of transporters in the intestine along the anterior-posterior and crypt-villus axes. BMC Genom. 6, 69.

Anders, S., Pyl, P.T., Huber, W., 2015. HTSeq–a Python framework to work with high-throughput sequencing data. Bioinformatics 31, 166–169.

Ang, S.L., Wierda, A., Wong, D., Stevens, K.A., Cascio, S., Rossant, J., Zaret, K.S., 1993. The formation and maintenance of the definitive endoderm lineage in the mouse: involvement of HNF3/forkhead proteins. Development 119, 1301–1315.

Barker, N., van Es, J.H., Kuipers, J., Kujala, P., van den Born, M., Cozijnsen, M., Haegebarth, A., Korving, J., Begthel, H., Peters, P.J., Clevers, H., 2007. Identification of stem cells in small intestine and colon by marker gene Lgr5. Nature 449, 1003–1007.

Basak, O., van de Born, M., Korving, J., Beumer, J., van der Elst, S., van Es, J.H., Clevers, H., 2014. Mapping early fate determination in Lgr5+ crypt stem cells using a novel Ki67-RFP allele. EMBO J. 33, 2057–2068.

Basak, O., Beumer, J., Wiebrands, K., Seno, H., van Oudenaarden, A., Clevers, H., 2017. Induced quiescence of Lgr5+ stem cells in intestinal organoids enables differentiation of hormone-producing enteroendocrine cells. Cell Stem Cell 20, 177–190.

Behrens, J., Jerchow, B.A., Würtele, M., Grimm, J., Asbrand, C., Wirtz, R., Kühl, M., Wedlich, D., Birchmeier, W., 1998. Functional interaction of an axin homolog, conductin, with beta-catenin, APC, and GSK3beta. Science 280, 596–599.

Beumer, J., Clevers, H., 2016. Regulation and plasticity of intestinal stem cells during homeostasis and regeneration. Development 143, 3639–3649.

Bowman, A.N., van Amerongen, R., Palmer, T.D., Nusse, R., 2013. Lineage tracing with Axin2 reveals distinct developmental and adult populations of Wnt/β-catenin-responsive neural stem cells. Proc. Natl. Acad. Sci. USA 110, 7324–7329.

Carmon, K.S., Gong, X., Lin, Q., Thomas, A., Liu, Q., 2011. Proc. Natl. Acad. Sci. USA 108, 11452–11457.

Chin, A.M., Hill, D.R., Aurora, M., Spence, J.R., 2017. Morphogenesis and maturation of the embryonic and postnatal intestine. Semin. Cell Dev. Biol. 66, 81–93.

Core Team, R., 2017. R: a language and environment for statistical computing. R. Found. Stat. Comput.https://www.R-project.org/.

Dobin, A., Davis, C.A., Schlesinger, F., Drenkow, J., Zaleski, C., Jha, S., Batut, P., Chaisson, M., Gingeras, T.R., 2013. STAR: ultrafast universal RNA-seq aligner. Bioinformatics 29, 15–21.

Fukuda, M., Mizutani, T., Mochizuki, W., Matsumoto, T., Nozaki, K., Sakamaki, Y., Ichinose, S., Okada, Y., Tanaka, T., Watanabe, M., Nakamura, T., 2014. Small intestinal stem cell identity is maintained with functional Paneth cells in heterotopically grafted epithelium onto the colon. Genes Dev. 28, 1752–1757.

Glinka, A., Dolde, C., Kirsch, N., Huang, Y.L., Kazanskaya, O., Ingelfinger, D., Boutros, M., Cruciat, C.M., Niehrs, C., 2011. LGR4 and LGR5 are R-spondin receptors mediating Wnt/beta-catenin and Wnt/PCP signalling. EMBO Rep. 12, 1055–1061.

Iwasaki, M., Tsuchiya, K., Okamoto, R., Zheng, X., Kano, Y., Okamoto, E., Okada, E., Araki, A., Suzuki, S., Sakamoto, N., Kitagaki, K., Akashi, T., Eishi, Y., Nakamura, T., Watanabe, M., 2011. Longitudinal cell formation in the entire human small intestine is correlated with the localization of Hath1 and Klf4. J. Gastroenterol. 46, 191–202.

Kazakevych, J., Sayols, S., Messner, B., Krienke, C., Soshnikova, N., 2017. Dynamic changes in chromatin states during specification and differentiation of adult intestinal stem cells. Nucleic Acids Res. 45, 5770–5784.

Kretzschmar, K., Clevers, H., 2017. Wnt/β-catenin signaling in adult mammalian epithelial stem cells. Dev. Biol. 428, 273–282.

Kwon, G.S., Viotti, M., Hadjantonakis, A.K., 2008. The endoderm of the mouse embryo arises by dynamic widespread intercalation of embryonic and extraembryonic lineages. Dev. Cell 15, 509–520.

de Lau, W., Barker, N., Low, T.Y., Koo, B.K., Li, V.S., Teunissen, H., Kujala, P., Haegebarth, A., Peters, P.J., van de Wetering, M., Stange, D.E., van Es, J.E., Guardavaccaro, D., Schasfoort, R.B., Mohri, Y., Nishimori, K., Mohammed, S., Heck, A.J., Clevers, H., 2011. Lgr5 homologues associate with Wnt receptors and mediate R-spondin signalling. Nature 476, 293–297.

Love, M.I., Huber, W., Anders, S., 2014. Moderated estimation of fold change and dispersion for RNA-seq data with DESeq. 2. Genome Biol. 15, 550.

Middendorp, S., Schneeberger, K., Wiegerinck, C.L., Mokry, M., Akkerman, R.D., van Wijngaarden, S., Clevers, H., Nieuwenhuis, E.E., 2014. Adult stem cells in the small intestine are intrinsically programmed with their location-specific function. Stem Cells 32, 1083–1091.

Nigmatullina, L., Norkin, M., Dzama, M.M., Messner, B., Sayols, S., Soshnikova, N., 2017. Id2 controls specification of Lgr5+ intestinal stem cell progenitors during gut development. EMBO J. 36, 869–885.

Park, E.J., Sun, X., Nichol, P., Saijoh, Y., Martin, J.F., Moon, A.M., 2008. System for tamoxifen-inducible expression of cre-recombinase from the Foxa2 locus in mice. Dev. Dyn. 2008 (237), 447–453.

Rawlins, E.L., Clark, C.P., Xue, Y., Hogan, B.L., 2009. The Id2+ distal tip lung epithelium contains individual multipotent embryonic progenitor cells. Development 136, 3741–3745.

Sherwood, R.I., Maehr, R., Mazzoni, E.O., Melton, D.A., 2011. Wnt signaling specifies and patterns intestinal endoderm. Mech. Dev. 128, 387–400.

Wang, X., Yamamoto, Y., Wilson, L.H., Zhang, T., Howitt, B.E., Farrow, M.A., Kern, F., Ning, G., Hong, Y., Khor, C.C., Chevalier, B., Bertrand, D., Wu, L., Nagarajan, N., Sylvester, F.A., Hyams, J.S., Devers, T., Bronson, R., Lacy, D.B., Ho, K.Y., Crum, C.P., McKeon, F., Xian, W., 2015. Cloning and variation of ground state intestinal stem cells. Nature 522, 173–178.